

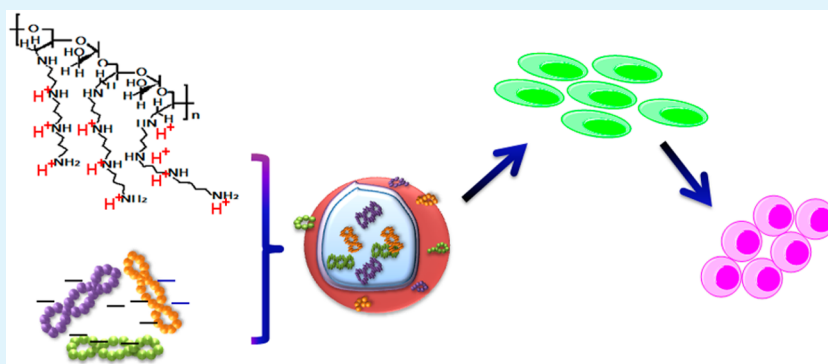
# MicroRNA Replacing Oncogenic Klf4 and c-Myc for Generating iPSC Cells via Cationized *Pleurotus eryngii* Polysaccharide-based Nanotransfection

Wenwen Deng,<sup>||,†</sup> Xia Cao,<sup>||,†</sup> Jingjing Chen,<sup>||,†</sup> Zhijian Zhang,<sup>‡</sup> Qingtong Yu,<sup>§</sup> Yan Wang,<sup>†</sup> Genbao Shao,<sup>‡</sup> Jie Zhou,<sup>†</sup> Xiangdong Gao,<sup>§</sup> Jiangnan Yu,<sup>\*,†</sup> and Ximing Xu<sup>\*,†</sup>

<sup>†</sup>Department of Pharmaceutics, School of Pharmacy, and Center for Drug/Gene Delivery and Tissue Engineering, Jiangsu University, Zhenjiang 212001, People's Republic of China

<sup>‡</sup>Center for Drug/Gene Delivery and Tissue Engineering, and School of Medical Science and Laboratory Medicine, Jiangsu University, Zhenjiang 212001, People's Republic of China

<sup>§</sup>School of Life Science & Technology, China Pharmaceutical University, Nanjing 210009, People's Republic of China



**ABSTRACT:** Induced pluripotent stem cells (iPSCs), resulting from the forced expression of cocktails out of transcription factors, such as Oct4, Sox2, Klf4, and c-Myc (OSKM), has shown tremendous potential in regenerative medicine. Although rapid progress has been made recently in the generation of iPSCs, the safety and efficiency remain key issues for further application. In this work, microRNA 302-367 was employed to substitute the oncogenic Klf4 and c-Myc in the OSKM combination as a safer strategy for successful iPSCs generation. The negatively charged plasmid mixture (encoding Oct4, Sox2, miR302-367) and the positively charged cationized *Pleurotus eryngii* polysaccharide (CPEPS) self-assembled into nanosized particles, named as CPEPS-OS-miR nanoparticles, which were applied to human umbilical cord mesenchymal stem cells for iPSCs generation after characterization of the physicochemical properties. The CPEPS-OS-miR nanoparticles possessed spherical shape, ultrasmall particle size, and positive surface charge. Importantly, the combination of plasmids Oct4, Sox2, and miR302-367 could not only minimize genetic modification but also show a more than 50 times higher reprogramming efficiency (0.044%) than any other single or possible double combinations of these factors (Oct4, Sox2, miR302-367). Altogether, the current study offers a simple, safe, and effective self-assembly approach for generating clinically applicable iPSCs.

**KEYWORDS:** induced pluripotent stem cells, microRNAs, nanoparticles, polysaccharides, self-assembly

## INTRODUCTION

Induced pluripotent stem cells (iPSCs) was first generated in 2006 when Yamanaka and Takahashi used a defined set of reprogramming factors: Oct4, Sox2, Klf4, and c-Myc (OSKM), which are commonly referred to as the “Yamanaka factors”,<sup>1,2</sup> to reprogram mouse embryonic fibroblast into a pluripotent state. Later, intense research provided the evidence that iPSCs could be derived from different species (human included) using various combinations from the transcription factors such as Oct4, Sox2, Klf4, c-Myc, Nanog, and Lin28.<sup>3</sup> These iPSCs share most of the characteristics with embryonic stem cells, including morphology, gene expression profiles, epigenetic modifications and pluripotency.<sup>4–6</sup> Therefore, iPSCs has opened up a new

horizon in the fields of disease modeling, drug screening, toxicology tests, and ultimately, autologous cell-based therapies.<sup>7–10</sup>

Currently, direct reprogramming by viral (retroviral and lentiviral) transduction of transcription factors is still the most commonly used procedures for iPSCs generation.<sup>11–13</sup> However, viral integration and spontaneous transgene reactivation may cause insertional mutagenesis and tumor formation, rendering the resultant iPSCs unqualified for clinical

**Received:** January 21, 2015

**Accepted:** August 13, 2015

**Published:** August 13, 2015

applications.<sup>14</sup> Searching for alternative strategy to induce pluripotency without incurring genetic change has thus become the focus of intense research effort. To this end, several strategies, such as excisable vectors,<sup>15</sup> reprogramming proteins,<sup>16</sup> microRNAs,<sup>17,18</sup> nonintegrating plasmids,<sup>19</sup> modified RNA, and RNA virus,<sup>20</sup> have been designed to avoid genomic modification as much as possible.

Even though somatic cells can be reprogrammed using different transcription factor cocktails, the original Yamanaka factors Oct4, Sox2, Klf4, and c-Myc remain the most frequently used cocktail for iPSC generation. Nevertheless, the two oncogenes c-Myc and Klf4 may cause undesirable genetic modification.<sup>21</sup> Significant effort has been made to develop approaches that avoid the use of these oncogenic transcription factors. It has been found that c-Myc is dispensable for reprogramming even though it enhances the efficiency and speed of reprogramming.<sup>22</sup> Furthermore, a recent study showed that transplantation of iPSCs without c-Myc in rats could alleviate retinal oxidative damage.<sup>23</sup> Likewise, Klf4 was found to be replaceable during the process of somatic cell reprogramming.<sup>24,25</sup> On the basis of viral strategies, some studies showed that human somatic cells could be reprogrammed into iPSCs with only Oct4 and Sox2.<sup>26</sup> However, on the basis of nonviral nanoparticulate gene delivery systems, whether iPSCs can be induced with a new combination without the oncogenes c-Myc and Klf4 still remains unknown.

Recently, several microRNAs (miRNAs) have been shown to enhance reprogramming efficiency when expressed along with the OSKM factors.<sup>27</sup> These miRNAs, which reside in clusters throughout the genome, belong to families of miRNAs that are expressed preferentially in embryonic stem cells (ESCs) and thought to help maintain ESC phenotype.<sup>28,29</sup> Of the miRNAs expressed at high levels in ESCs, the cluster 302-367 (miR302-367) was reported to be able to increase the iPSC generation efficiency in the presence of several of the OSKM factors by targeting TGF- $\beta$  receptor 2, promoting E-cadherin expression and accelerating mesenchymal-to-epithelial transition which is necessary for iPSC colony formation.<sup>30</sup> Recent studies found that miR302/367 cluster played pivotal roles during the process of the somatic cell reprogramming.<sup>31–33</sup> However, as mentioned above, these advanced strategies still needed viral vehicles, and using nonviral systems for miRNA-mediated iPSC generation has not yet been explored.

Owing to the extremely low transfection efficiency of naked nucleic acids, it is crucial to develop safe, simple, and efficient gene carriers. Biomaterials that can safely and efficiently deliver these transcription factors hold the potential to achieve somatic cell reprogramming. Cationic polymers, especially naturally occurring polysaccharides, showed great promise as materials for efficient nonviral gene delivery due to their excellent biocompatibility, low immunogenicity, efficient gene encapsulation, promotion of cellular uptake and facilitation of endosomal escape, which would allow for DNA release in the cytoplasm.<sup>34–37</sup> An emerging nonviral carrier material cationized *Pleurotus eryngii* polysaccharide (CPEPS) was produced by cationic modification of a naturally occurring polysaccharide extracted from the edible mushroom *Pleurotus eryngii* and showed excellent capacity to encapsulate plasmid DNA to form self-assembled nanoparticles, which could efficiently transfect rat bone marrow mesenchymal stem cells.<sup>38</sup> In addition, the self-assembly synthetic strategy based on the electrostatic interactions not only enables control upon the assembly behavior which further determines the sizes, zeta

potentials, surface chemistry and payloads of the resultant particles but also protects the nucleic acids from nuclease in the environment, opening up numerous ways for biomedical applications.<sup>39,40</sup>

In this study, the negatively charged plasmids, encoding Oct4, Sox2, and miR302-367, alone and in all possible double and triple combinations with each other (resulting in a total of seven different compositions) mixed with the positively charged CPEPS, and the two oppositely charged components self-assembled into nanoparticles. As a result, nanoparticles prepared with the combination of Oct4, Sox2, and miR302-367 showed highest reprogramming efficiency in human umbilical cord mesenchymal stem cells (HUMSCs), a type of somatic stem cell that could be an ideal parental cell source due to their accessibility and low immunogenicity, as well as their associated less invasive and painless procedures and lower risk of viral contamination.<sup>41</sup>

Here, for the first time, miR302-367 was used to replace the two oncogenic factors Klf4 and c-Myc in the original OSKM combination and the CPEPS was applied for the first time as well in the field of human iPSC generation. The oppositely charged plasmids and CPEPS self-assembled into CPEPS-OS-miR nanoparticles driven by the electrostatic interactions, providing a simple, safe and effective self-assembly approach for generating clinically applicable iPSCs.

## MATERIALS AND METHODS

**Materials.** Fetal bovine serum (FBS), Dulbecco's modified Eagle's medium (DMEM), DMEM/F12, knockout DMEM, knockout serum replacement (KSR), bovine serum albumin, L-glutamine, penicillin, streptomycin and trypsin were obtained from Gibco BRL (Invitrogen Co., Carlsbad, CA). Aphidicolin, type IV collagenase,  $\beta$ -mercaptoethanol, nonessential amino acids and basic fibroblast growth factor (bFGF) were purchased from Sigma-Aldrich (St. Louis, MO).

The *Pleurotus eryngii* polysaccharide was isolated and chemically modified to obtain the cationized *Pleurotus eryngii* polysaccharide (CPEPS) according to the procedure reported in our previous study.<sup>38</sup> According to this report, the CPEPS has an average molecular weight of 333 kDa, with the total amount of nitrogen being  $3.92 \pm 0.23 \mu\text{mol}$  per microgram of CPEPS.

The use of experimental animals adhered to the principles in the Declaration of Helsinki. The animal experimental protocols were approved by the University Ethics Committee for the use of experimental animals and human samples.

**Plasmid Preparation.** The three individual plasmids encoding Oct4, Sox2 and miR302-367 were purchased from GeneCopeia, Inc. (Rockville, MD) and were then amplified in *Escherichia coli* host strain DH5 $\alpha$ . The plasmids DNA were then extracted and purified by column chromatography with the PureYield Plasmid Maxiprep Start-Up Kit (Promega, Madison, WI) according to the instructions provided by the manufacturer. The antibiotic ampicillin was used to select the plasmids-transformed *E. coli* cells. The concentration of each plasmid DNA was quantified by measuring the UV absorbance at 260 nm with an ultraviolet spectrophotometer (Shimadzu, Tokyo, Japan). Using the original plasmids as controls, the agarose electrophoresis was conducted to verify each plasmid extracted from *E. coli* cells.

**Preparation of CPEPS-OS-miR Nanoparticles.** Equal amounts of the three plasmids (Oct4 and Sox2, and miR302-367) were mixed together to obtain a plasmid mixture solution. A 2 mg/mL CPEPS solution and the plasmid mixture solution were heated separately at 55 °C for 30 min. Next, the polysaccharide solution was added to the plasmid mixture, followed by vortexing for 30 s to obtain CPEPS-OS-miR nanoparticles. Nanoparticles with various weight ratios of CPEPS/plasmids (1:1, 5:1, 10:1, 20:1, 30:1, and 50:1) were prepared as described above and then applied to an agarose gel for electrophoresis to assess the binding effect between the CPEPS and the plasmids. From the electrophoresis pattern, we selected the

optimal weight ratio, and the nanoparticles prepared with this optimal weight ratio were used in the follow-up experiments.

**Characterization of CPEPS-OS-miR Nanoparticles.** The morphology of CPEPS-OS-miR nanoparticles was observed under a transmission electron microscopy (TEM) (JEM-2100, JEOL, Japan). The zeta potential and particle size of CPEPS-OS-miR nanoparticle solution was measured with a Malvern Instruments ZEN3600 Nano Series Zetasizer (Malvern Instruments, Ltd., UK).

The encapsulation efficiency of CPEPS-OS-miR nanoparticles was determined using the method in previous studies.<sup>42,43</sup> Briefly, the nanoparticle samples were prepared and centrifuged at 16,000 g for 50 min to separate the nanoparticles from the aqueous medium containing free plasmid DNA. The concentration of the free plasmid in the clear supernatant was measured with a UV spectrometry (BioSpec-mini, Shimadzu Co., Tokyo, Japan). The calibration curve was performed in phosphate-buffered saline (PBS, pH 7.4). The encapsulation is defined as

$$\varepsilon(\%) = \frac{W_0 - W_1}{W_0} \times 100\%$$

where  $W_0$  is the total amount of the plasmids that were used for preparing nanoparticles, and  $W_1$  is the amount of free plasmids.

**Cell Culture and iPSC Generation.** Primary HUMSCs, provided by Beike Jiangsu Stem Cell Bank (Taizhou, China), were maintained in the low glucose DMEM supplemented with 10% FBS and 100 U/mL penicillin-streptomycin. Mouse embryonic fibroblasts (MEFs) were purchased from the Cell Bank at the Chinese Academy of Science (Shanghai, China) and cultured in the fibroblast medium: DMEM/F12 containing 10% FBS and 100 U/mL penicillin-streptomycin.

One day before transfection, HUMSCs were seeded on a 24-well plate at a density of  $1 \times 10^5$  cells/mL (0.5 mL suspension per well) and were maintained in DMEM (containing 10% FBS and 100 U/mL penicillin-streptomycin) at 37 °C and 5% CO<sub>2</sub>. When the cells reached 80–90% confluence, the medium was replaced with serum-free DMEM containing CPEPS-OS-miR nanoparticles and nanoparticles which prepared with single or any possible combinations of two factors out of Oct4, Sox2 and miR302-367 have been conducted for transfection according to the same protocol. In total, 0.4 μg of plasmids was applied in each well. Four hours later, the medium was replaced with fresh serum containing DMEM. The same transfection procedure was conducted on day 2, 4, and 6. During the treatment with CPEPS-OS-miR nanoparticles, we also added 600 nM aphidicolin according to the published work.<sup>44</sup> On day 7, the transfected HUMSCs were treated with 1 mg/mL type IV collagenase at 37 °C for 30 min. After centrifugation (1500 rpm for 5 min), the cells were seeded on the mitomycin C-treated MEF feeder layers at a density of  $1 \times 10^3$  cells/mL in the following human ESC (hESC) medium: knockout DMEM supplemented with 20% KSR, 2 mmol/L L-glutamine, 0.1 mmol/L β-mercaptoethanol, 1% nonessential amino acids, 4 ng/mL bFGF, and 100 U/mL penicillin-streptomycin. The medium was replaced daily with fresh prewarmed hESC medium. The colony development was observed every day under a microscope.

**Cytotoxicity Examination.** The cytotoxicity of CPEPS-OS-miR nanoparticles (with ratios of 5:1, 10:1, 20:1, and 50:1) was examined with MTT (3-(4,5-dimethyl-2-thiazyl)-2,5-diphenyl-2H-tetrazolium bromide) assay according the procedures in previous study.<sup>34</sup> Lipofectamine2000 was used as control, and the measured absorbance was normalized to the absorbance of the nontreated control cells.

**RNA Preparation and qRT-PCR Analysis.** To quantify the transfection efficiency and the expression of pluripotent markers in the induced cells, qRT-PCR analysis was conducted to examine the RNA levels of each factor, including Sox2, Oct4, Klf4, c-Myc, Nanog, SSEA4, and miR302-367. After the final transfection with CPEPS-OS-miR, CPEPS-OSKM, and Lipofectamine2000-OS-miR, the total RNAs were extracted using TRIzol reagent (Invitrogen Co., Carlsbad, CA) following the manufacturer's instructions. Quantitative PCR was conducted using SYBR Premix Ex Taq (TaKaRa, Shiga, Japan) according to the protocols provided by the manufacturer with the LightCycler system (Roche Molecular Biochemicals, Indianapolis, IN).

GAPDH was used as an internal standard. Primer sequences were as follows: GAPDH forward, CGGAGTCAACGGATTTGGTCGTAT; GAPDH reverse, AGCCTTCTCCATGGTGGTGAAGAC; Sox2 forward, GCCCTGCAGTACAACCTCCAT; Sox2 reverse, GACTTG-ACCACCGAACCCAT; Oct4 forward, ATGTGGTCCGAGTGTG-GTTC; Oct4 reverse, AAACCTGGCACAACCTCCA; c-Myc forward, CGTCCTCGGATCTCTGTCTC; c-Myc reverse, GCTGGTGCATTTTCGGTTGT; Klf4 forward, GGAATCGCT-TCATGTGGGA; Klf4 reverse, GGAATCGCTTCATGTGGGA; Nanog forward, GAGATGCCTCACACGGAGAC; Nanog reverse, CTTTGGGACTGGTGGGAAGAA; SSEA4 forward, TGGACG-GGCACAACCTCATC; SSEA4 reverse, GGGCAGGTTCTTGG-CACTCA; miR302-367 forward, CGCGGATCCAGGACTACT-TTCCCCAGAGC; and miR302-367 reverse, CCGCTCGAG-TTTAACCAGTTAACCACAAC.

**Alkaline Phosphatase (AP) Staining and Determination of Reprogramming Efficiency.** For AP staining, the cells were washed twice with PBS, fixed in precooled 4% paraformaldehyde for 2 min, and washed again with PBS. The AP activity was examined using the BCIP/NBT Alkaline Phosphatase Color Development Kit (Blue) (C3206, Beyotime Institute of Biotechnology, Haimen, China)<sup>5</sup> according to the manufacturer's instructions. The images were acquired using microscopy (Olympus, Tokyo).

The reprogramming efficiency was calculated as the number of iPSC colonies formed per number of cells seeded for transfection. The iPSC colonies were identified on the basis of ESC-like morphology, and AP staining was used to facilitate the identification of iPSC colonies.

**Immunofluorescence Staining.** Immunostaining was conducted to examine the expression of pluripotent markers. Cells were fixed in 4% paraformaldehyde in PBS for 20 min. After being washed twice with PBS, the cells were permeabilized with 0.1% Triton X-100 for 10 min. After another washing with PBS, the cells were incubated in 4% bovine serum albumin for 1 h to block any nonspecific binding. The cells were then incubated with the primary antibodies overnight at 4 °C. After being washed with PBS, the cells were incubated with secondary antibodies for 2 h at room temperature. Nuclei were counterstained with 4',6-diamidino-2-phenylindole (DAPI, 1:2000; Sigma, St. Louis, MO). The primary antibodies included anti-Nanog (1:250), anti-Oct-4 (1:250), anti-SSEA-3 (1:250), anti-SSEA-4 (1:250), and anti-Tra-1-81 (1:250), which were obtained from Abcam (Cambridge, MA). The secondary antibody was goat antimouse IgG-Cy3, obtained from Sigma, at a dilution ratio of 1:500. The fluorescence was detected using a Leica epifluorescence light microscope (Leica Microsystems, Wetzlar, Germany).

**Teratoma Formation.** To determine the developmental pluripotency, we injected the iPSCs into immunocompromised mice for teratoma formation. These experiments were approved by the University Ethics Committee for the Use of Experimental Animals and adhered to the Guidelines for the Care and Use of Laboratory Animals. Briefly, the iPSCs were washed with PBS and detached with type IV collagenase for 30 min at 37 °C. The cells were collected by centrifugation and were then resuspended in hESC medium at a density of  $1 \times 10^7$  cells/mL. A 100-μL aliquot of the cell suspension was subcutaneously injected into four-week-old immunocompromised nonobese diabetic/severe combined immunodeficient (NOD/SCID) mice (Comparative Medicine Center, Yangzhou University, Yangzhou, China). Eight weeks after the cell injection, the teratomas were collected and processed for Western blot analysis with antibodies against smooth muscle actin (SMA, a mesoderm marker), βIII tubulin (an ectoderm marker), and α-fetoprotein (AFP, an endoderm marker).

**Statistical Analysis.** Quantitative data are presented as the means ± standard derivations (SDs). Data were analyzed using the statistical software package SPSS 16.0 (SPSS Inc., Chicago, IL).

## RESULTS

**Fabrication of CPEPS-OS-miR Nanoparticles.** To optimize the weight ratio of CPEPS/plasmids, we subjected

these nanoparticles to the agarose gel electrophoresis. Figure 1 shows the pattern of plasmid migration across the gel.

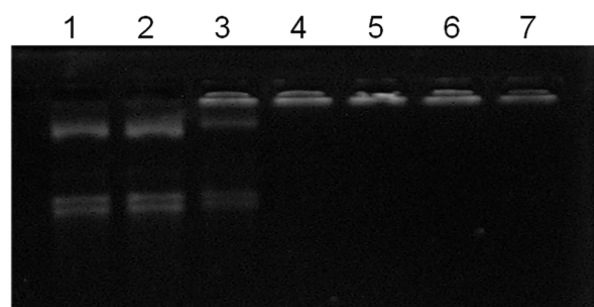


**Figure 1.** Gel retardation assay of CPEPS-OS-miR nanoparticles in 1% agarose gel. Lane 1: mixture of free plasmids Oct4, Sox2, and miR302-367. Lanes 2–7: CPEPS-OS-miR nanoparticles prepared with CPEPS/plasmids weight ratios of 1:1, 5:1, 10:1, 20:1, 30:1, and 50:1, respectively.

Obviously, the gel retardation effect increased as the CPEPS/plasmids weight ratio increased. In particular, when the CPEPS/plasmids weight ratio was 10:1 (Lane 4 in Figure 1), there was no sign of plasmid migration, indicating a strong and stable binding between the CPEPS and plasmids. Additionally,

we evaluated the encapsulation efficiency of CPEPS-OS-miR nanoparticles produced at this weight ratio. The data resulting from five different batches of CPEPS-OS-miR nanoparticles showed an average encapsulation efficiency of approximately 99.2%, demonstrating that the nanoparticles with the CPEPS/plasmids weight ratio of 10:1 can completely condense the plasmid mixture. Thus, the CPEPS-OS-miR nanoparticles described in the following experiments were prepared at the CPEPS/plasmids weight ratio of 10:1 unless otherwise noted.

**Characterization of CPEPS-OS-miR Nanoparticles.** The morphology of the CPEPS-OS-miR nanoparticles was observed under transmission electronic microscope (TEM). As shown in Figure 2A, CPEPS-OS-miR nanoparticles possessed a relatively homogeneous spherical shape with particle size ranging from 40 to 100 nm. The particle size of CPEPS-OS-miR nanoparticles was further determined with the dynamic light scattering (DLS) analysis, and the results demonstrated that these nanoparticles had an average particle size of 112 nm (Figure 2B), which was slightly larger than that of the TEM result. This phenomenon is common and has been widely recognized because samples were detected in different conditions with DLS and TEM, that is, the nanoparticles were in suspended solution when measured by DLS technique, whereas dried particles were observed by TEM.<sup>43,45</sup>

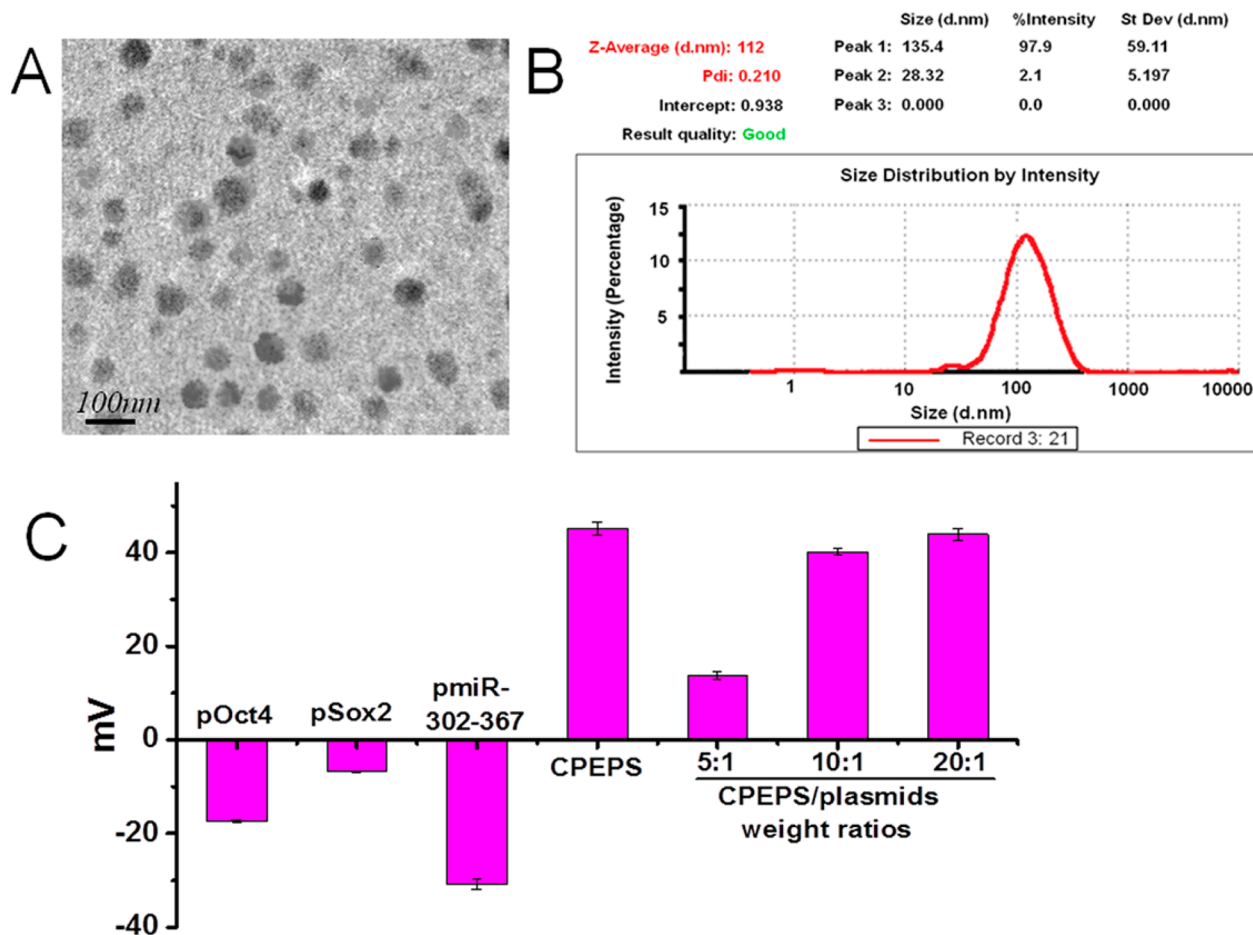


**Figure 2.** Characterization of the CPEPS-OS-miR nanoparticles. (A) TEM image of the CPEPS-OS-miR nanoparticles. (B) Size distribution pattern of CPEPS-OS-miR nanoparticles determined with dynamic light scattering technique. (C) Zeta potential of the three individual free plasmids Oct4 (bar 1), Sox2 (bar 2), miR302-367 (bar 3), CPEPS (bar 4), and CPEPS-OS-miR nanoparticles prepared with weight ratios of (left to right) 5:1, 10:1, and 20:1). Data are mean  $\pm$  standard deviation (SD,  $n = 3$ ).

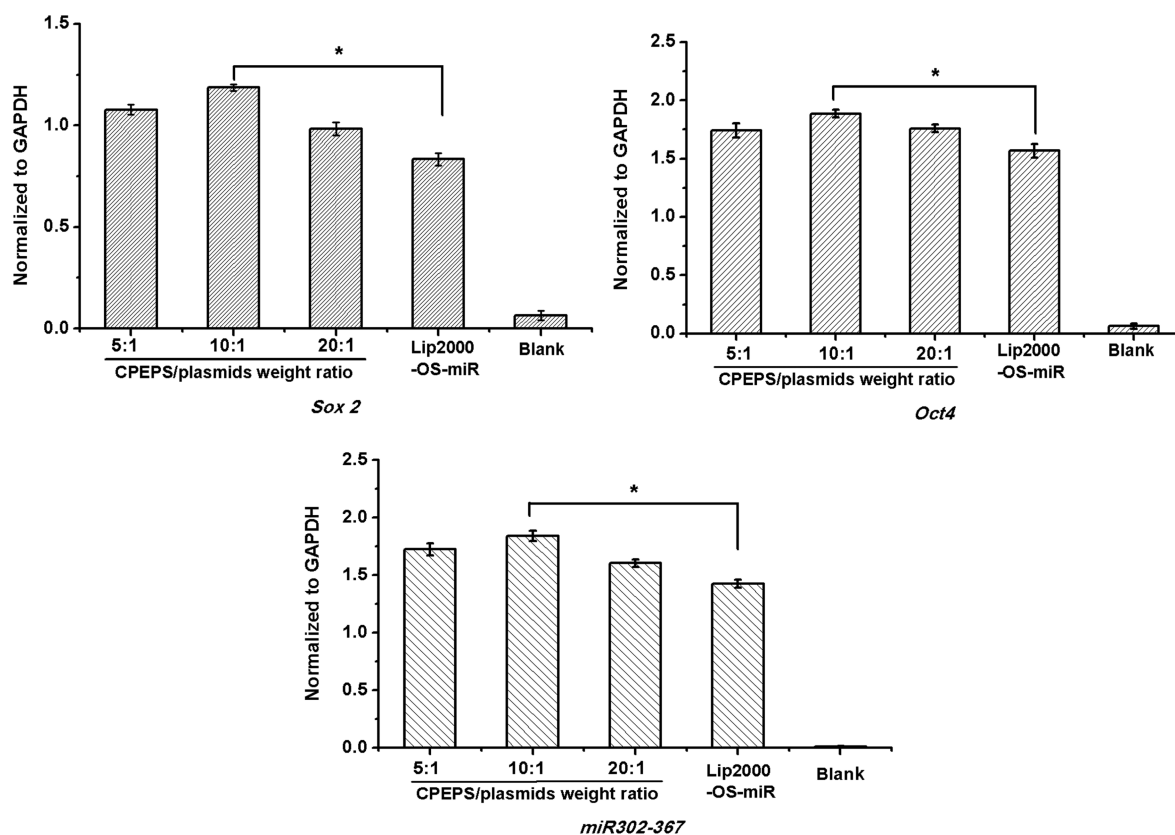


**Figure 3.** QRT-PCR analysis for the expression of Sox2, Oct4 and miR302-367 in the transfected cells. CPEPS-OS-miR nanoparticles prepared with three different weight ratios (5:1, 10:1, and 20:1) were examined; the standard transfection reagent Lipofectamine2000 was used as positive control and the cells with no treatment were the negative control. Gene expressions were normalized by GAPDH ( $n = 3$ , mean  $\pm$  standard deviation; \*,  $p < 0.05$ , Student's  $t$  test).

The results of the zeta potential analyses were illustrated in Figure 2C. The CPEPS showed a positive charge as expected ( $+45.30 \pm 0.17$  mV), and all the three plasmids exhibited negative potentials: ( $-17.40 \pm 0.08$ ) mV for pOct4, ( $-6.81 \pm 0.06$ ) mV for pSox2, and ( $-30.80 \pm 0.13$ ) mV for pmir302-367. When complexed with the positively charged CPEPS, the zeta potential of the plasmid mixture exhibited a reversed from negative to positive. Notably, when the CPEPS/plasmid weight ratio increased from 5:1 to 20:1, the zeta potential increased from  $\sim +13$  to  $\sim +40$  mV, suggesting that the positive zeta potential increased as the CPEPS/plasmid weight ratio increased.

**Determination of Transfection Efficiency.** The transfection efficiency was quantified with qRT-PCR. CPEPS-OS-miR nanoparticles with three different CPEPS/plasmids weight ratios (5:1, 10:1, and 20:1) were assessed, using the widely recognized standard transfection reagent, Lipofectamine2000, as positive control. As shown in Figure 3, after four consecutive transfections, CPEPS-OS-miR nanoparticles with ratio of 10:1 showed significantly higher expression levels of Sox2, Oct4, and miR302-367 compared with Lipofectamine2000 ( $p < 0.05$ , Student's  $t$  test). Consistently, CPEPS-OS-miR nanoparticles prepared at the weight ratio of 10:1 displayed obviously greater transfection efficiency than those prepared with CPEPS/plasmids weight ratios of 5:1 and 20:1. These data indicate that CPEPS-OS-miR nanoparticles with the weight ratio of 10:1 are the optimal candidate for gene delivery.

**Cytotoxicity Evaluation.** An ideal gene vector should be nontoxic to cells. In this study, CPEPS-OS-miR nanoparticles

prepared with various CPEPS/plasmids weight ratios (5:1, 10:1, 20:1, and 50:1) have been evaluated. As a result, all the CPEPS-OS-miR nanoparticles showed higher cell viability than Lipofectamine2000 (Figure 4). Particularly, CPEPS-OS-miR nanoparticles with weight ratios of 5:1 and 10:1 displayed comparable cell viability to the nontreated cells, indicating excellent compatibility of CPEPS-OS-miR nanoparticles which were prepared with lower CPEPS/plasmids weight ratios;

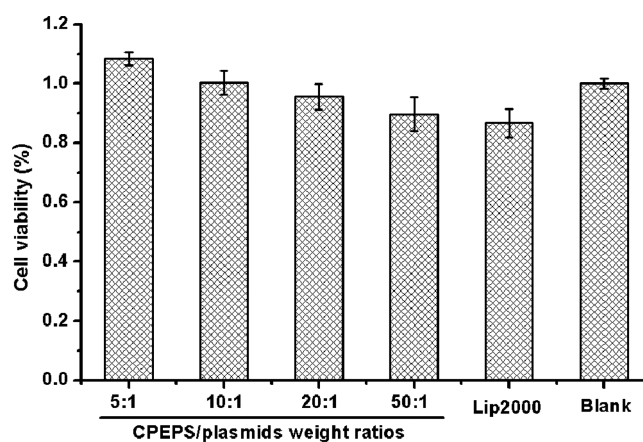


**Figure 4.** Cell viability assay. CPEPS-OS-miR nanoparticles with weight ratios of 5:1, 10:1, 20:1, and 50:1 were tested; the standard transfection reagent Lipofectamine2000 was employed as control. The cell viability percentage was normalized to the blank group (nontreated cells). Data are mean  $\pm$  standard deviation (SD,  $n = 3$ ).

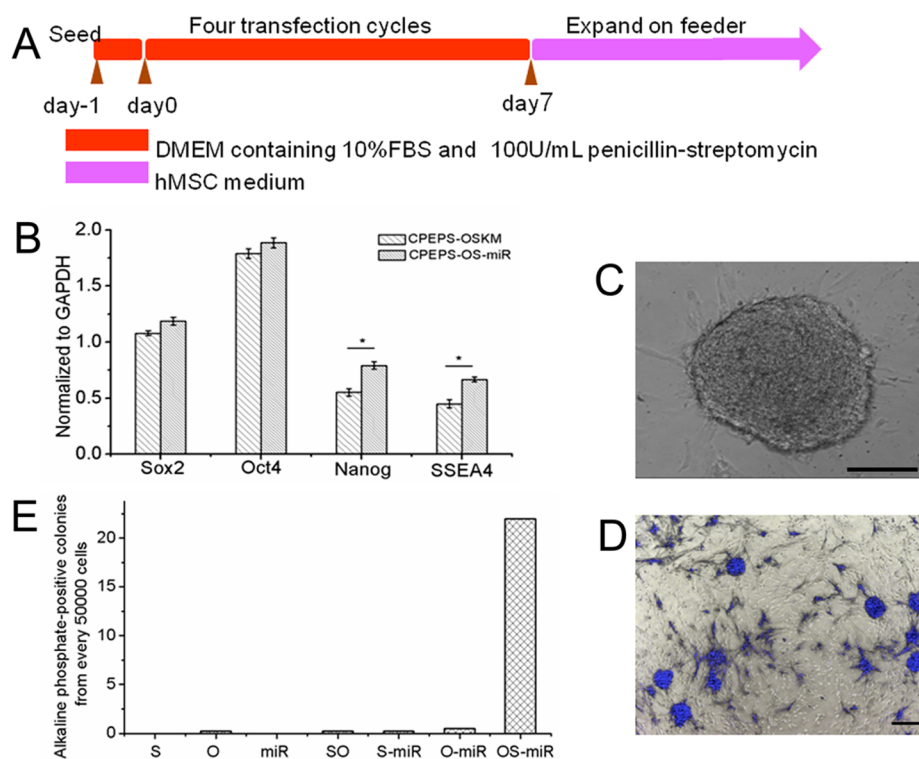


**Figure 5.** Generation of iPSCs. (A) Timeline of iPSC production with four cycles of consecutive transfection. (B) qRT-PCR analysis for the expression of pluripotency markers, including Sox2, Oct4, Nanog, and SSEA4, in the induced cells. Gene expressions were normalized by GAPDH ( $n = 3$ , mean  $\pm$  standard deviation; \*,  $p < 0.05$ , Student's  $t$  test). (C) A phase-contrast image of iPSC colonies on day 12, magnification  $\times 200$ ; scale bar = 200  $\mu\text{m}$ . (D) IPSC colonies stained for alkaline phosphatase activity, magnification  $\times 100$ ; scale bar = 100  $\mu\text{m}$ . (E) Quantification of alkaline phosphatase-positive colonies in all seven possible combinations from the three factors (S, Sox2; O, Oct4; and miR, miR302-367).

however, as the CPEPS/plasmids weight ratio went up (such as 20:1 and 50:1), there was a gradual decline in cell viability. Nevertheless, even those with higher CPEPS/plasmids weight ratios (such as 50:1) showed greater cell viability than Lipofectamine2000.

**Reprogramming HUMSCs with CPEPS-OS-miR Nanoparticles.** For generation of iPSCs, CPEPS-OS-miR nanoparticles were incubated with HUMSCs following the timeline depicted in Figure 5A. It is well established that the reprogramming process generally required 8–12 days,<sup>46</sup> thus four consecutive transfection cycles (transfection on day 0, day 2, day 4, and day 6) was conducted in this study. To further compare the reprogramming efficiency, nanoparticles which prepared with single or any possible two-factor combinations out of Oct4, Sox2 and miR302-367 have been conducted for transfection according to the same protocol. During the treatment with these nanoparticles, we also added 600 nM aphidicolin according to the published work.<sup>44</sup> One day after final transfection (day 7), part of the induced cells were seeded on the MEFs feeder layers in hESC medium; others were proceeded with qRT-PCR analysis for the evaluation of pluripotent markers, including Sox2, Oct4, Nanog, and SSEA4. As shown in Figure 5B, as compared to the CPEPS-OSKM complex, CPEPS-OS-miR nanoparticles showed enhanced expression of Sox2 and Oct4 as well as significantly increased level of Nanog and SSEA4 ( $p < 0.05$ , Student's  $t$  test). Several colonies (more than 10) of ESC-like morphology (Figure 5C) were observed 6 days after final transfection (day 12) in the group treated with CPEPS-OS-miR nanoparticles, while only one or two ESC-like morphology colonies formed in other groups, most of which could not steadily expand on

feeder layers. Alkaline phosphatase (AP) has been established as a marker for embryonic stem cells. We therefore tested the presence of AP when the iPSC colonies were passaged onto MEFs layers at day 15 and counted the number of the blue-stained colonies in each group by day 29. As a result, only the combination of Oct4, Sox2, and miR302-367 generated an average of 22 colonies with a typical AP-staining pattern that was restricted to the iPSC colonies (Figure 5D) from  $5 \times 10^4$  cells; other six combinations showed none, one or two AP-positive colonies from  $2 \times 10^5$  cells, most of which could not stably expanded on feeder layers. This result showed the remarkably greater reprogramming of the triple-factor combination in comparison with other possible groups (Figure 5E).

To verify the proliferation inhibition effect of aphidicolin on iPSC formation, HUMSCs were transfected in parallel with CPEPS-OS-miR nanoparticles with or without aphidicolin. The group of CPEPS-OS-miR nanoparticles with aphidicolin formed 22 colonies on day 29. These colonies could be stably passaged while maintaining the ESC-like morphology. However, only 3 ESC-like colonies appeared in the group without aphidicolin treatment, which soon became automatically differentiated (data not shown). This result confirmed the findings from a previous study,<sup>44</sup> in which aphidicolin was found to be beneficial for generating of iPSCs.

**Pluripotent Properties of iPSCs.** After the ESC-like iPSCs were split onto feeder layers, iPSC colonies formed; then, immunofluorescence was conducted to detect the expression of pluripotent markers, including Tra-1-81, SSEA-3, SSEA-4, Nanog, and Oct4. As shown in Figure 6, antibodies specific to these marker proteins positively stained the tested iPSC colonies, indicating that pluripotency was successfully

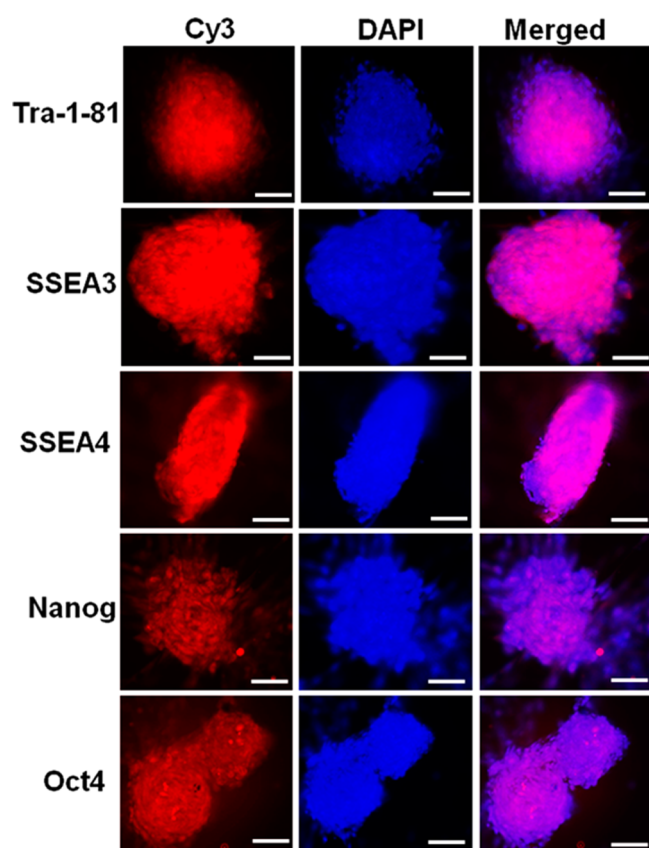


**Figure 6.** Immunofluorescence staining assays for the expression of the pluripotency marker genes in iPSCs. Cellular expressions of pluripotency markers Tra-1-81, SSEA-3, SSEA-4, Nanog, and Oct4, all of which are human ESC makers observed in the iPSCs. The nuclei were stained with DAPI (blue), magnification  $\times 200$ ; scale bar = 50  $\mu\text{m}$ .

induced by the four consecutive transfections with the CPEPS-OS-miR nanoparticles.

**Differentiation Potential of iPSCs.** Furthermore, the developmental potential of the established iPSCs was evaluated via teratoma formation in suspension culture for 3 days. The iPSC colonies were collected and injected into NOD/SCID mice. Well-encapsulated cystic tumors initially appeared one month later. The tumors were allowed to develop for an additional month, and protein expression in the teratomas was then evaluated in Western blots. As shown in Figure 7, the teratoma tissues were positive against the three-germ layer

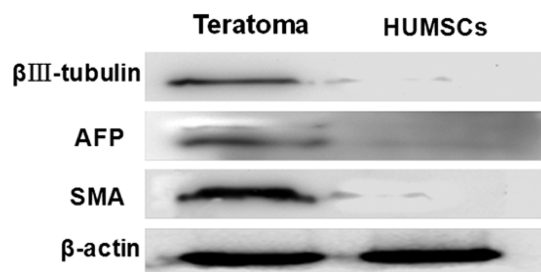


**Figure 7.** In vivo developmental potential of iPSCs. The Western blot pattern shows the expression of the three germ layers in the teratoma, including  $\beta$ III tubulin (an ectoderm marker), AFP (an endoderm marker), and SMA (a mesoderm marker), and  $\beta$ -actin was used as the loading control.

markers, including  $\beta$ III tubulin (ectoderm), AFP (endoderm), and SMA (mesoderm), while no expression of three germ layer markers was observed in the control group, HUMSCs. This result confirms the differentiation potential of the CPEPS-OS-miR nanoparticle-generated iPSCs into three germ lineages.

## DISCUSSION

Although numerous nonviral strategies have been developed for generating iPSCs, the naturally occurring polysaccharide appears to be the superior option due to its unique advantages such as biodegradability, biocompatibility, nontoxicity and the feasibility of chemical modification. In this study, the *Pleurotus eryngii* polysaccharide was isolated and cationically modified to obtain the cationized *Pleurotus eryngii* polysaccharide, that is CPEPS, according to the procedure reported in our previous study.<sup>38</sup> CPEPS-OS-miR nanoparticles with a series of weight ratios (CPEPS/plasmids, 1:1, 5:1, 10:1, 20:1, 30:1, 50:1) was prepared according to the previous method with slight modification.<sup>38</sup> The results of agarose gel electrophoresis showed that the CPEPS-OS-miR nanoparticles had a good gel retardation effect. Moreover, the high encapsulation efficiency (99.2%) indicated the strong capacity of the CPEPS to carry plasmid DNAs.

It is well-known that particle size and shape are very important factors for cellular uptake because they affect the pathways and efficiency of internalization. It has been reported that nanoparticles of  $<200$  nm size exhibited the best properties for cellular uptake,<sup>47</sup> and our nanoparticles fell within this range. Previous studies also showed that sphere-shaped nanoparticles had a higher efficiency of cellular uptake than rod- and needle-shaped nanoparticles.<sup>48,49</sup> These findings support the fact that CPEPS-OS-miR nanoparticles possessed a small particle size and spherical shape, which were preferable for internalization.

Surface charge is another important factor for uptake because the cell membrane consists of a bilayer of lipid and anionic membrane proteins, which are helpful for the uptake of cationic complexes.<sup>50</sup> In this study, the CPEPS-OS-miR nanoparticles were formed by self-assembly of the oppositely charged CPEPS and plasmids mixture in aqueous solution.<sup>51</sup> To examine the surface charge of the self-assembled nanoparticles, zeta potential analysis was conducted. As a result, the CPEPS-OS-miR nanoparticles had positive charges, which not only can facilitate the encapsulation of the plasmids, but also may benefit the process of approaching cell membrane.<sup>52</sup> These results demonstrated that the CPEPS-OS-miR nanoparticles possessed favorable attributes for cellular uptake, which will benefit reprogramming.

It is interesting that CPEPS-OS-miR nanoparticles with a weight ratio of 10:1 possessed the highest transfection efficiency when compared with nanoparticles of other weight ratios (5:1 and 20:1). The possible reason is that when the weight ratio is smaller than 10:1, the cationic polysaccharide is not enough for complete encapsulation of plasmids and when greater than 10:1, the excessive amount of positively charge CPEPS might result in cytotoxicity as shown in the cytotoxicity assay (Figure 4). Even though the cell viability slightly declined when CPEPS-OS-miR nanoparticles were prepared at greater weight ratios (such as 50:1), it was still higher than that of Lipofectamine2000. This result indicates the sound safety of CPEPS-OS-miR nanoparticles, which may be an important reason for the enhanced transfection efficiency in comparison with Lipofectamine2000 (Figure 3).

Most importantly, colonies with ESC-like morphology appeared as early as 6 days after the final transfection, the reprogramming kinetics of this method were significantly accelerated compared to that of many nonviral strategies<sup>53,54</sup> and even viral methods.<sup>55</sup> Delightfully, the reprogramming efficiency of the current strategy reached 0.044%. Although the reprogramming efficiency of the current CPEPS-OS-miR nanoparticles was not higher than our previous work, the reprogramming speed of CPEPS-OS-miR nanoparticles (colonies first appear 6 days after the final transfection) was notably faster than the previously reported Yamanaka factors-encapsulated calcium phosphate nanoparticles (colonies first appear 23 days after the final transfection).<sup>19</sup> These data demonstrate that CPEPS-OS-miR nanoparticles with aphidicolin could reprogram HUMSCs to pluripotency in a fast and highly efficient manner.

Furthermore, nanoparticles prepared with single or any possible two-factor combinations of Oct4, Sox2, and miR302-367 have been employed for iPSC generation with the same protocol. As a result, the CPEPS-OS-miR nanoparticles showed a more than 50 fold higher reprogramming efficiency and remarkably faster speed of iPSC induction than others.

The AP staining and immunofluorescence results demonstrated the positive expression of the pluripotency markers. When injected into the flanks of the NOD/SCID mice, the iPSCs could form teratomas that positively express the three-germ layer markers, including  $\beta$ III tubulin (ectoderm), AFP (endoderm), and SMA (mesoderm). These data support the conclusion that CPEPS-OS-miR nanoparticles can successfully reprogram HUMSCs into a pluripotent state in a simple and efficient manner.

## CONCLUSIONS

In summary, we herein report a new cocktail containing Oct4, Sox2, and miR302-367 that was selected from seven different compositions due to its highest reprogramming efficiency. The CPEPS deriving from the naturally occurring *Pleurotus eryngii* polysaccharide and the plasmids encoding Oct4, Sox2, and miR302-367 self-assembled into nanosized particles. The CPEPS-OS-miR nanoparticles were spherical in shape and small in particle size and possessed a positive zeta potential. Six days after the final transfection, the iPSC colonies appeared, and a total of 22 colonies from the 50 000 originally seeded cells were counted on day 29 (efficiency 0.044%). The iPSCs closely resemble ESCs with respect to morphology, pluripotency, and differentiation capacity. This is first report that describes the application of *Pleurotus eryngii* polysaccharide as the nonviral vector for iPSCs generation via the new combination of Oct4, Sox2, and miR302-367. These findings indicate that the self-assembly CPEPS-OS-miR nanoparticles provide a novel, simple, safe, and effective alternative for generating of iPSCs that are desirable for clinical application.

## AUTHOR INFORMATION

### Corresponding Authors

\*E-mail: [xmxu@ujs.edu.cn](mailto:xmxu@ujs.edu.cn). Tel/Fax: +86-511-85038451.

\*E-mail: [yjn@ujs.edu.cn](mailto:yjn@ujs.edu.cn). Tel/Fax: +86-511-88797078.

### Author Contributions

<sup>||</sup>W.W.D. and X.C. performed the experiments; W.W.D., X.C. and J.J.C. contributed equally to this work. W.W.D. completed data analysis and wrote the manuscript; J.J.C., Y.W., Q.T.Y., and J.Z. performed cell and tissue culture; Z.J.Z. assisted with image

analysis and evaluation; G.B.S. and X.D.G. provided technical assistance; J.N.Y. contributed in developing the concept of the one-time transfection strategy; X.M.X. designed and directed the study and edited the paper. The manuscript was written through contributions of all authors. All authors have given approval for the final version of the manuscript. These authors contributed equally to this work.

### Funding

This work was supported by National Natural Science Foundation of China (81072586, 81273470, and 81473172), Doctoral Fund of Ministry of Education of China (20123227110009), and Special Funds for 333 projects (BRA2013198) and Industry–University–Research Institution Cooperation (JHB2012-37, GY2012049, GY2013055) in Jiangsu Province and Zhenjiang City. Senior professionals' foundation of Jiangsu University projects (13JDG007) and A Project Funded by the Priority Academic Program Development of Jiangsu Higher Education Institutions.

### Notes

The authors declare no competing financial interest.

## ACKNOWLEDGMENTS

We are grateful to Dr. Yuan Wei at Jiangsu University for purchasing the plasmids and Beike Jiangsu Stem Cell Bank (Taizhou, China) for providing HUMSCs isolation.

## ABBREVIATIONS

hESCs	human embryonic stem cells
iPSCs	induced pluripotent stem cells
CPEPS	cationized <i>Pleurotus eryngii</i> polysaccharide
ESC	embryonic stem cell
NOD/SCID	nonobese/severe combined immunodeficiency
OS	Oct4 and Sox2
HUMSCs	human umbilical cord mesenchymal stem cells
miRNAs	microRNAs
miR302-367	miRNAs 302-367
CPEPS-OS-miR nanoparticles	the negatively charged plasmid mixture (encoding Oct4, Sox2, miR302-367) and the positively charged cationized <i>Pleurotus eryngii</i> polysaccharide (CPEPS) self-assemble into nanosized particles
AP	alkaline phosphatase
AFP	$\alpha$ -fetoprotein
SMA	$\alpha$ -smooth muscle actin
TEM	transmission electronic microscope

## REFERENCES

- (1) Takahashi, K.; Yamanaka, S. Induction of Pluripotent Stem Cells from Mouse Embryonic and Adult Fibroblast Cultures by Defined Factors. *Cell* **2006**, *126*, 663–676.
- (2) Chiou, S.-H.; Jang, S.-F.; Mou, C.-Y. Mesoporous Silica Nanoparticles: A Potential Platform for Generation of Induced Pluripotent Stem Cells? *Nanomedicine* **2014**, *9*, 377–380.
- (3) Yu, J.; Vodyanik, M. A.; Smuga-Otto, K.; Antosiewicz-Bourget, J.; Frane, J. L.; Tian, S.; Nie, J.; Jonsdottir, G. A.; Ruotti, V.; Stewart, R. Induced Pluripotent Stem Cell Lines Derived from Human Somatic Cells. *Science* **2007**, *318*, 1917–1920.



- (4) Aasen, T.; Raya, A.; Barrero, M. J.; Garreta, E.; Consiglio, A.; Gonzalez, F.; Vassena, R.; cacute, J. B.; Pekarik, V.; Tiscornia, G.; Edel, M. Efficient and Rapid Generation of Induced Pluripotent Stem Cells from Human Keratinocytes. *Nat. Biotechnol.* **2008**, *26*, 1276–1284.
- (5) Hochedlinger, K.; Plath, K. Epigenetic Reprogramming and Induced Pluripotency. *Development* **2009**, *136*, 509–523.
- (6) Park, I.-H.; Zhao, R.; West, J. A.; Yabuuchi, A.; Huo, H.; Ince, T. A.; Lerou, P. H.; Lensch, M. W.; Daley, G. Q. Reprogramming of Human Somatic Cells to Pluripotency with Defined Factors. *Nature* **2008**, *451*, 141–146.
- (7) Kang, H.; Shih, Y.-R. V.; Hwang, Y.; Wen, C.; Rao, V.; Seo, T.; Varghese, S. Mineralized Gelatin Methacrylate-Based Matrices Induce Osteogenic Differentiation of Human Induced Pluripotent Stem Cells. *Acta Biomater.* **2014**, *10*, 4961–4970.
- (8) Lee, Y.-K.; Ng, K.-M.; Tse, H.-F. Modeling of Human Cardiomyopathy with Induced Pluripotent Stem Cells. *J. Biomed. Nanotechnol.* **2014**, *10*, 2562–2585.
- (9) Drawnel, F. M.; Boccardo, S.; Prummer, M.; Delobel, F.; Graff, A.; Weber, M.; Gerard, R.; Badi, L.; Kam-Thong, T.; Bu, L.; Jiang, X.; Hoflack, J.-C.; Kiiialainen, A.; Jeworutzki, E.; Aoyama, N.; Carlson, C.; Burcin, M.; Gromo, G.; Boehringer, M.; Stahlberg, H.; Hall, B. J.; Magnone, M. C.; Kolaja, K.; Chien, K. R.; Bailly, J.; Iacone, R. Disease Modeling and Phenotypic Drug Screening for Diabetic Cardiomyopathy Using Human Induced Pluripotent Stem Cells. *Cell Rep.* **2014**, *9*, 810–820.
- (10) Willard, V. P.; Diekman, B. O.; Sanchez-Adams, J.; Christoforou, N.; Leong, K. W.; Guilak, F. Use of Cartilage Derived from Murine Induced Pluripotent Stem Cells for Osteoarthritis Drug Screening. *Arthritis Rheumatol.* **2014**, *66*, 3062–3072.
- (11) Maherali, N.; Ahfeldt, T.; Rigamonti, A.; Utikal, J.; Cowan, C.; Hochedlinger, K. A High-Efficiency System for the Generation and Study of Human Induced Pluripotent Stem Cells. *Cell Stem Cell* **2008**, *3*, 340–345.
- (12) Takahashi, K.; Tanabe, K.; Ohnuki, M.; Narita, M.; Ichisaka, T.; Tomoda, K.; Yamanaka, S. Induction of Pluripotent Stem Cells from Adult Human Fibroblasts by Defined Factors. *Cell* **2007**, *131*, 861–872.
- (13) Chen, C.-L.; Wang, L.-J.; Yan, Y.-T.; Hsu, H.-W.; Su, H.-L.; Chang, F.-P.; Hsieh, P. C. H.; Hwang, S.-M.; Shen, C.-N. Cyclin D1 Acts as a Barrier to Pluripotent Reprogramming by Promoting Neural Progenitor Fate Commitment. *FEBS Lett.* **2014**, *588*, 4008–4017.
- (14) Okita, K.; Ichisaka, T.; Yamanaka, S. Generation of Germline-Competent Induced Pluripotent Stem Cells. *Nature* **2007**, *448*, 313–317.
- (15) Carey, B. W.; Markoulaki, S.; Hanna, J.; Saha, K.; Gao, Q.; Mitalipova, M.; Jaenisch, R. Reprogramming of Murine and Human Somatic Cells Using a Single Polycistronic Vector. *Proc. Natl. Acad. Sci. U. S. A.* **2009**, *106*, 157–162.
- (16) Kim, D.; Kim, C.-H.; Moon, J.-I.; Chung, Y.-G.; Chang, M.-Y.; Han, B.-S.; Ko, S.; Yang, E.; Cha, K. Y.; Lanza, R. Generation of Human Induced Pluripotent Stem Cells by Direct Delivery of Reprogramming Proteins. *Cell Stem Cell* **2009**, *4*, 472–476.
- (17) Judson, R. L.; Babiarz, J. E.; Venere, M.; Belloch, R. Embryonic Stem Cell-Specific MicroRNAs Promote Induced Pluripotency. *Nat. Biotechnol.* **2009**, *27*, 459–461.
- (18) Miyoshi, N.; Ishii, H.; Nagano, H.; Haraguchi, N.; Dewi, D. L.; Kano, Y.; Nishikawa, S.; Tanemura, M.; Mimori, K.; Tanaka, F. Reprogramming of Mouse and Human Cells to Pluripotency Using Mature MicroRNAs. *Cell Stem Cell* **2011**, *8*, 633–638.
- (19) Cao, X.; Deng, W.; Qu, R.; Yu, Q.; Li, J.; Yang, Y.; Cao, Y.; Gao, X.; Xu, X.; Yu, J. Non-Viral Co-Delivery of the Four Yamanaka Factors for Generation of Human Induced Pluripotent Stem Cells Via Calcium Phosphate Nanocomposite Particles. *Adv. Funct. Mater.* **2013**, *23*, 5403–5411.
- (20) Mormone, E.; D'Sousa, S.; Alexeeva, V.; Bederson, M. M.; Germano, I. M. "Footprint-Free" Human Induced Pluripotent Stem Cell-Derived Astrocytes for in Vivo Cell-Based Therapy. *Stem Cells Dev.* **2014**, *23*, 2626–2636.
- (21) Nakagawa, M.; Koyanagi, M.; Tanabe, K.; Takahashi, K.; Ichisaka, T.; Aoi, T.; Okita, K.; Mochiduki, Y.; Takizawa, N.; Yamanaka, S. Generation of Induced Pluripotent Stem Cells without Myc from Mouse and Human Fibroblasts. *Nat. Biotechnol.* **2007**, *26*, 101–106.
- (22) Wernig, M.; Meissner, A.; Cassady, J. P.; Jaenisch, R. C-Myc Is Dispensable for Direct Reprogramming of Mouse Fibroblasts. *Cell Stem Cell* **2008**, *2*, 10–12.
- (23) Fang, I. M.; Yang, C.-H.; Chiou, S.-H.; Yang, C.-M. Induced Pluripotent Stem Cells without C-Myc Ameliorate Retinal Oxidative Damage Via Paracrine Effects and Reduced Oxidative Stress in Rats. *J. Ocul. Pharmacol. Ther.* **2014**, *30*, 757–770.
- (24) Feng, B.; Jiang, J.; Kraus, P.; Ng, J.-H.; Heng, J.-C. D.; Chan, Y.-S.; Yaw, L.-P.; Zhang, W.; Loh, Y.-H.; Han, J. Reprogramming of Fibroblasts into Induced Pluripotent Stem Cells with Orphan Nuclear Receptor Esrrb. *Nat. Cell Biol.* **2009**, *11*, 197–203.
- (25) Chen, J.; Liu, J.; Yang, J.; Chen, Y.; Chen, J.; Ni, S.; Song, H.; Zeng, L.; Ding, K.; Pei, D. Bmps Functionally Replace Klf4 and Support Efficient Reprogramming of Mouse Fibroblasts by Oct4 Alone. *Cell Res.* **2011**, *21*, 205–212.
- (26) Giorgetti, A.; Montserrat, N.; Aasen, T.; Gonzalez, F.; Rodríguez-Pizà, I.; Vassena, R.; Raya, A.; Boué, S.; Barrero, M. J.; Corbella, B. A. Generation of Induced Pluripotent Stem Cells from Human Cord Blood Using Oct4 and Sox2. *Cell Stem Cell* **2009**, *5*, 353–357.
- (27) James, E. N.; Delany, A. M.; Nair, L. S. Post-Transcriptional Regulation in Osteoblasts Using Localized Delivery of Mir-29a Inhibitor from Nanofibers to Enhance Extracellular Matrix Deposition. *Acta Biomater.* **2014**, *10*, 3571–3580.
- (28) Wang, Y.; Belloch, R. Cell Cycle Regulation by MicroRNAs in Embryonic Stem Cells. *Cancer Res.* **2009**, *69*, 4093–4096.
- (29) Wang, Y.; Baskerville, S.; Shenoy, A.; Babiarz, J. E.; Baehner, L.; Belloch, R. Embryonic Stem Cell-Specific MicroRNAs Regulate the G1-S Transition and Promote Rapid Proliferation. *Nat. Genet.* **2008**, *40*, 1478–1483.
- (30) Liao, B.; Bao, X.; Liu, L.; Feng, S.; Zovoilis, A.; Liu, W.; Xue, Y.; Cai, J.; Guo, X.; Qin, B. MicroRNA Cluster 302-367 Enhances Somatic Cell Reprogramming by Accelerating a Mesenchymal-to-Epithelial Transition. *J. Biol. Chem.* **2011**, *286*, 17359–17364.
- (31) Anokye-Danso, F.; Trivedi, C. M.; Juhr, D.; Gupta, M.; Cui, Z.; Tian, Y.; Zhang, Y.; Yang, W.; Gruber, P. J.; Epstein, J. A. Highly Efficient Mirna-Mediated Reprogramming of Mouse and Human Somatic Cells to Pluripotency. *Cell Stem Cell* **2011**, *8*, 376–388.
- (32) Wang, L.; Zhu, H.; Wu, J.; Li, N.; Hua, J. Characterization of Embryonic Stem-Like Cells Derived from Hek293t Cells through Mir302/367 Expression and Their Potentiality to Differentiate into Germ-Like Cells. *Cytotechnology* **2014**, *66*, 729–740.
- (33) Zhang, Z.; Xiang, D.; Heriyanto, F.; Gao, Y.; Qian, Z.; Wu, W.-S. Dissecting the Roles of Mir-302/367 Cluster in Cellular Reprogramming Using Tale-Based Repressor and Talen. *Stem Cell Rep.* **2013**, *1*, 218–225.
- (34) Deng, W. W.; Cao, X.; Wang, M.; Yang, Y.; Su, W. Y.; Wei, Y. W.; Ou-Yang, Z.; Yu, J. N.; Xu, X. M. Efficient Gene Delivery to Mesenchymal Stem Cells by an Ethylenediamine-Modified Polysaccharide from Mulberry Leaves. *Small* **2012**, *8*, 441–451.
- (35) Xu, X.; Capito, R. M.; Spector, M. Delivery of Plasmid IGF-1 to Chondrocytes Via Cationized Gelatin Nanoparticles. *J. Biomed. Mater. Res., Part A* **2008**, *84*, 73–83.
- (36) Liu, Y.; Wang, Y.; Zhang, C.; Zhou, P.; Liu, Y.; An, T.; Sun, D.; Zhang, N.; Wang, Y. Core-Shell Nanoparticles Based on Pullulan and Poly(B-Amino) Ester for Hepatoma-Targeted Codelivery of Gene and Chemotherapy Agent. *ACS Appl. Mater. Interfaces* **2014**, *6*, 18712–18720.
- (37) Zhao, Y.; Yu, B.; Hu, H.; Hu, Y.; Zhao, N.-N.; Xu, F.-J. New Low Molecular Weight Polycation-Based Nanoparticles for Effective Codelivery of Pdna and Drug. *ACS Appl. Mater. Interfaces* **2014**, *6*, 17911–17919.
- (38) Deng, W. W.; Cao, X.; Wang, M.; Qu, R.; Su, W. Y.; Yang, Y.; Wei, Y. W.; Xu, X. M.; Yu, J. N. Delivery of a Transforming Growth

Factor B-1 Plasmid to Mesenchymal Stem Cells Via Cationized Pleurotus eryngii Polysaccharide Nanoparticles. *Int. J. Nanomed.* **2012**, *7*, 1297–1311.

(39) Liu, Y.; Wang, H.; Kamei, K. i.; Yan, M.; Chen, K. J.; Yuan, Q.; Shi, L.; Lu, Y.; Tseng, H. R. Delivery of Intact Transcription Factor by Using Self-Assembled Supramolecular Nanoparticles. *Angew. Chem.* **2011**, *123*, 3114–3118.

(40) Goldberger, J. E.; Berns, E. J.; Bitton, R.; Newcomb, C. J.; Stupp, S. I. Electrostatic Control of Bioactivity. *Angew. Chem., Int. Ed.* **2011**, *50*, 6292–6295.

(41) Lu, L.-L.; Liu, Y.-j.; Yang, S.-G.; Zhao, Q.-J.; Wang, X.; Gong, W.; Han, Z.-B.; Xu, Z.-S.; Lu, Y.-X.; Liu, D. Isolation and Characterization of Human Umbilical Cord Mesenchymal Stem Cells with Hematopoiesis-Supportive Function and Other Potentials. *Haematologica* **2006**, *91*, 1017–1026.

(42) Zhao, K.; Shi, X.; Zhao, Y.; Wei, H.; Sun, Q.; Huang, T.; Zhang, X.; Wang, Y. Preparation and Immunological Effectiveness of a Swine Influenza DNA Vaccine Encapsulated in Chitosan Nanoparticles. *Vaccine* **2011**, *29*, 8549–8556.

(43) Deng, W.; Fu, M.; Cao, Y.; Cao, X.; Wang, M.; Yang, Y.; Qu, R.; Li, J.; Xu, X.; Yu, J. *Angelica Sinensis* Polysaccharide Nanoparticles as Novel Non-Viral Carriers for Gene Delivery to Mesenchymal Stem Cells. *Nanomedicine* **2013**, *9*, 1181–1191.

(44) Xu, Y.; Wei, X.; Wang, M.; Zhang, R.; Fu, Y.; Xing, M.; Hua, Q.; Xie, X. Proliferation Rate of Somatic Cells Affects Reprogramming Efficiency. *J. Biol. Chem.* **2013**, *288*, 9767–9778.

(45) Suzuki, M.; Shinkai, M.; Kamihira, M.; Kobayashi, T. Preparation and Characteristics of Magnetite-Labelled Antibody with the Use of Poly (Ethylene Glycol) Derivatives. *Biotechnol. Appl. Biochem.* **1995**, *21*, 335–345.

(46) Stadtfeld, M.; Nagaya, M.; Utikal, J.; Weir, G.; Hochedlinger, K. Induced Pluripotent Stem Cells Generated without Viral Integration. *Science* **2008**, *322*, 945–949.

(47) Yin Win, K.; Feng, S.-S. Effects of Particle Size and Surface Coating on Cellular Uptake of Polymeric Nanoparticles for Oral Delivery of Anticancer Drugs. *Biomaterials* **2005**, *26*, 2713–2722.

(48) Chithrani, B. D.; Ghazani, A. A.; Chan, W. C. Determining the Size and Shape Dependence of Gold Nanoparticle Uptake into Mammalian Cells. *Nano Lett.* **2006**, *6*, 662–668.

(49) Chithrani, B. D.; Chan, W. C. Elucidating the Mechanism of Cellular Uptake and Removal of Protein-Coated Gold Nanoparticles of Different Sizes and Shapes. *Nano Lett.* **2007**, *7*, 1542–1550.

(50) Chen, W.; Tsai, P.-H.; Hung, Y.; Chiou, S.-H.; Mou, C.-Y. Nonviral Cell Labeling and Differentiation Agent for Induced Pluripotent Stem Cells Based on Mesoporous Silica Nanoparticles. *ACS Nano* **2013**, *7*, 8423–8440.

(51) Wang, F.; Liu, Z.; Wang, B.; Feng, L.; Liu, L.; Lv, F.; Wang, Y.; Wang, S. Multi-Colored Fibers by Self-Assembly of DNA, Histone Proteins, and Cationic Conjugated Polymers. *Angew. Chem.* **2014**, *126*, 434–438.

(52) Piest, M.; Engbersen, J. F. Effects of Charge Density and Hydrophobicity of Poly (Amido Amine) S for Non-Viral Gene Delivery. *J. Controlled Release* **2010**, *148*, 83–90.

(53) Kaji, K.; Norrby, K.; Paca, A.; Mileikovsky, M.; Mohseni, P.; Woltjen, K. Virus-Free Induction of Pluripotency and Subsequent Excision of Reprogramming Factors. *Nature* **2009**, *458*, 771–775.

(54) Bhise, N. S.; Wahlin, K. J.; Zack, D. J.; Green, J. J. Evaluating the Potential of Poly (Beta-Amino Ester) Nanoparticles for Reprogramming Human Fibroblasts to Become Induced Pluripotent Stem Cells. *Int. J. Nanomed.* **2013**, *8*, 4641–4658.

(55) Takahashi, K.; Okita, K.; Nakagawa, M.; Yamanaka, S. Induction of Pluripotent Stem Cells from Fibroblast Cultures. *Nat. Protoc.* **2007**, *2*, 3081–3089.